Estimating the Impact of Gas Flaring Sites on the Air Quality and Environment Sustainability in Kirkuk City Using GIS Techniques

Deeman Salahaldeen Noori
Department of Surveying Engineering Techniques, Technical Engineering College of Kirkuk, Northern Technical University, Kirkuk, Iraq
deman.salahdeen24gs@ntu.edu.iq (corresponding author)

Nada Subhi Abdulmajeed
Department of Architecture and Construction Engineering Techniques, Technical Engineering College of Kirkuk, Northern Technical University, Kirkuk, Iraq
nst_architect@ntu.edu.iq

Received: 25 April 2025 | Revised: 20 May 2025 | Accepted: 6 June 2025

 DOI: https://doi.org/10.48084/etasr.11706

ABSTRACT

Gas flaring poses a significant environmental challenge, impacting air quality and exacerbating global warming. This research evaluates the impact of gas flaring on the air quality and environmental sustainability of Kirkuk City, utilizing Geographic Information System (GIS) techniques, the Analytical Hierarchy Process (AHP) with classification methods, and Gaussian Plume Dispersion Modeling (GPDM). Experts apply Pasquill-Gifford stability classes and dispersion parameters to model SO_2, NO_2, and PM pollutants. The GIS-based AHP method identifies priority contamination areas by evaluating various environmental and health factors. The classification systems enhance spatial analysis by pinpointing hazardous locations based on pollutant levels and their proximity to gas vent sites. Research findings indicate that pollution levels are highest near flaring sites, primarily due to atmospheric conditions that influence the dispersion of pollutants. The Gaussian Plume Model (GPM) shows that pollution levels decrease with distance from the source; however, densely populated areas can still experience unsafe levels. AHP results indicate that urban areas have the greatest impact, with a weight of 0.545, while vegetation has a significant effect on the environment, with a weight of 0.364. Barren land contributes the least to environmental risk, with a multiplier of only 0.091. This study develops a comprehensive framework that combines GIS decision-making techniques with dispersion models to assist policymakers in addressing environmental issues caused by gas flaring. It demonstrates that maintaining environmental regulations and proper planning are crucial for reducing air pollution threats in Kirkuk City and beyond.

Keywords-Gaussian plume model; air pollution; AHP; GIS; remote sensing

I. INTRODUCTION

Gas flaring involves burning natural gas that accompanies crude oil, often due to the lack of proper technology to utilize the gas. There is considerable gas flaring in Kirkuk, resulting in greenhouse gas emissions and deteriorating air quality [2]. Additionally, flaring releases hazardous toxins, including sulfur dioxide, nitrogen oxides, and volatile organic compounds, which have a negative impact on the health of nearby communities [3-4]. The population in residential areas, especially in Kirkuk, is most impacted by the proximity of homes to oil fields and refineries, as well as the effects of gas flaring [5]. Some communities complain of respiratory problems, skin rashes, and other health issues, attributing the incidents to polluting gases released during flaring. Such health risks most often affect children and the elderly. Additionally, the ongoing combustion of gas results in lighting up the surroundings and emitting heat, thus serving as a constant reminder that drifts through nearby communities [7]. The environmental impact of flaring in Kirkuk is also concerning; the main effect resulting from this flaring is the release of gases into the environment [8]. It plays a crucial role in the formation of acid rain, which damages the soil, water, and plants [9-10]. A study that used dispersive modeling, supported by GIS, in Turkey found that GIS enhances how we visualize and make decisions about air pollution control. Like Kirkuk, combining weather data and emission sources helped identify vulnerable areas [11]. In India, a combination of GIS-based air pollution models is used to investigate how pollutants from industrial plants spread in the area [12]. Additionally, a study was conducted on gas flaring and its effects around the Niger Delta, using GIS [13].

Analysis in Kirkuk revealed that the North Oil Company (NOC) is the primary source of pollution, accounting for approximately 80% of emissions [14]. It manages many oil fields with gas flaring towers, but these frequently lack efficient filters, adding to atmospheric pollution [15]. As a result, air quality has worsened, with residents reporting foul odors and health issues [16]. Analysis of air pollutant density in Kirkuk using GIS tools has proven beneficial [8, 17]. Research indicates that the air quality index in Kirkuk falls within the unhealthy to hazardous range, with PM10 particles ranging from 300 to 570 µg/m³ and PM2.5 levels of 40-60 µg/m³ [14]. It is crucial to respond promptly when addressing pollution sources that harm the environment [18]. Additional GIS studies in areas near the main entrance routes and oil facilities, especially the NOC, where the average annual PM10 emission rates in Kirkuk were estimated at nearly 120.8 µg/m³, indicating high levels beyond the safe standards, and highlighting the contribution of industrialization and transportation sources to air pollution [19].

A GIS is a computer-assisted technology used in acquiring, storing, processing, analyzing, managing, and displaying all types of geographic information [20-21]. Thus, GIS applications merge traditional database functions, such as queries and statistical calculations, with the core benefits of maps [22]. These capabilities distinguish GIS from other information systems and make GIS valuable in various organizations, both public and private, for describing events, predicting outcomes, and planning [23]. It should be emphasized that map making and geographic analysis, in general, are not new, but a GIS performs both tasks more quickly and with much greater precision [24]. In essence, the key factor is how effectively these tools have been integrated to provide a seamlessly deployable, functional geographic data processing system [25]. The usefulness of GIS lies in its ability to input, store, and analyze spatial data, as well as to respond to spatial queries [26].

The World Bank promotes its "Zero Routine Flaring by 2030" initiative, fostering meaningful collaborations between governments, businesses, and communities [27]. Sustainable environment goals require changes in social viewpoints about both energy development and usage methods [28]. Reducing dependence on fossil fuels and flaring requires three main initiatives: implementing renewable energy systems, adopting energy efficiency measures, and making ongoing investments in sustainable networks [29]. The public needs to understand environmental issues, and communities must actively participate because both aspects promote stakeholder responsibility and emphasize environmental protection [30]. Kirkuk City faces issues related to gas flaring, which pollutes the air and jeopardizes sustainable urban growth. This investigation is crucial for understanding the environmental issues associated with gas flaring in Kirkuk City, particularly in relation to public health and sustainability. Therefore, this research aims to assess the impact of gas flaring sites on air quality and the sustainable environment in Kirkuk City, utilizing GIS tools and the GPM for spatial and temporal analysis. Using GIS tools, gas flaring locations around Kirkuk City were identified to assess their impact and proximity to human settlements. Additionally, the study involved evaluating the density of pollutant gases and particulates generated by these flaring activities with the assistance of the GPM. Thus, we can assess how gas flaring impacts the sustainable development of Kirkuk City, particularly in terms of its effects on vegetation and urban growth.

II. STUDY AREA

The study area is located in the northeast part of Kirkuk City, situated between the coordinates 35° 24' – 35° 30' N and 44° 21' – 40° 27' E. Figure 1 represents the gas flaring site in Kirkuk City.

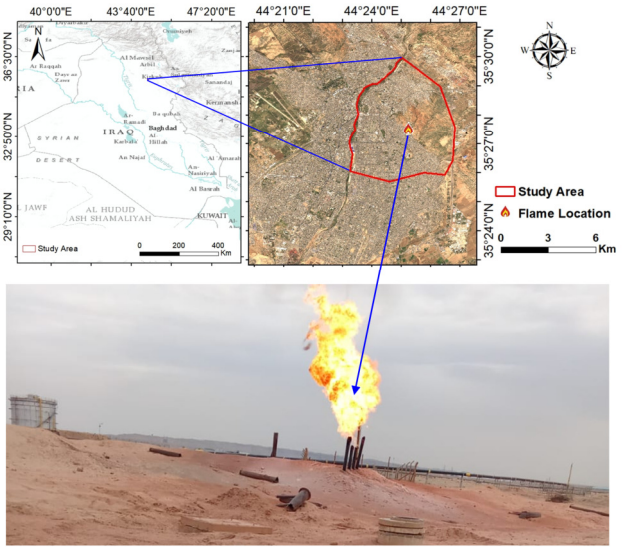

Fig. 1. Gas flaring location in the study area, Kirkuk City.

Kirkuk city in Iraq has become a serious environmental and health problem because of gas flaring, which is common in oil-exporting countries. Kirkuk has long been a hub of oil exploration and refining, primarily due to its substantial oil reserves. However, the negative effects of this industrial activity, including gas flaring from crude oil extraction, threaten the city's environment and public health, hindering its efforts toward sustainable development.

III. STUDY DATA AND PROCESSING

The study combines multiple data sources, including satellite imagery from Sentinel-2, air pollution metrics, and meteorological data, to evaluate the impact of gas flaring on air quality in Kirkuk City. The analysis utilizes detailed satellite imagery to classify land use, identify locations of gas flaring sites, and monitor environmental conditions. Accumulated air pollution data includes measurements of sulfur dioxide (SO_2), nitrogen oxides (NO_2), and particulate matter (PM) collected through ground-based monitoring stations and specialized data collection devices. Table I shows the specifications of the Sentinel-2 image. Figure 2 illustrates the map of the Sentinel-2 image used for classification. Additionally, wind speed data have been generated using Python to create Wind Rose diagrams, as shown in Figure 3.

TABLE I. SPECIFICATIONS OF THE SENTINEL-2 IMAGE

Platform name	Sentinel-2 L2A
Date of sensing	01/12/2024
Cloud cover	0.00572 %
Image resolution	10 m
Acquisition mode	INS-NOBS
Coordinate system	WGS-1984

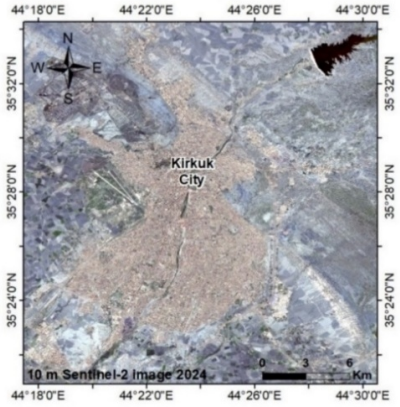

Fig. 2. Sentinel-2 image-based map of Kirkuk City.

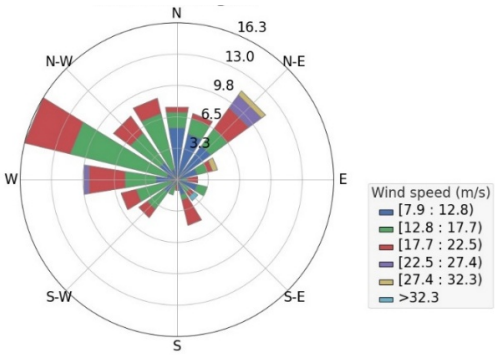

Fig. 3. Wind Rose diagram.

The GPM considers the emission rate (Q), representing the amount of pollutant released into the atmosphere during a specific time frame. This data can be sourced from emission monitoring systems or estimated using emission factors provided by environmental agencies for different fuel types and usage. Alternatively, it can be calculated by multiplying the pollutant concentration at the source, the gas exit velocity, and the cross-sectional area of the stack or flaring point.

Multiple datasets serve as vital information for validating the GPDM and pinpointing polluted areas. An accurate pollutant dispersion model relies heavily on meteorological data such as wind speed and direction. Data processing involves the use of ArcGIS software, Python programming, and statistical analysis. GIS is used to integrate datasets, facilitating a detailed pollution risk assessment that highlights vulnerable zones and supports the formulation of sustainable air quality management plans for Kirkuk city. The data collected in 2024 is split into two periods: summer and winter.

IV. METHODOLOGY

This study includes three main stages in its methodology: area classification, application of the GPDM, and GIS-based pollution risk mapping. Figure 4 illustrates the research methodology.

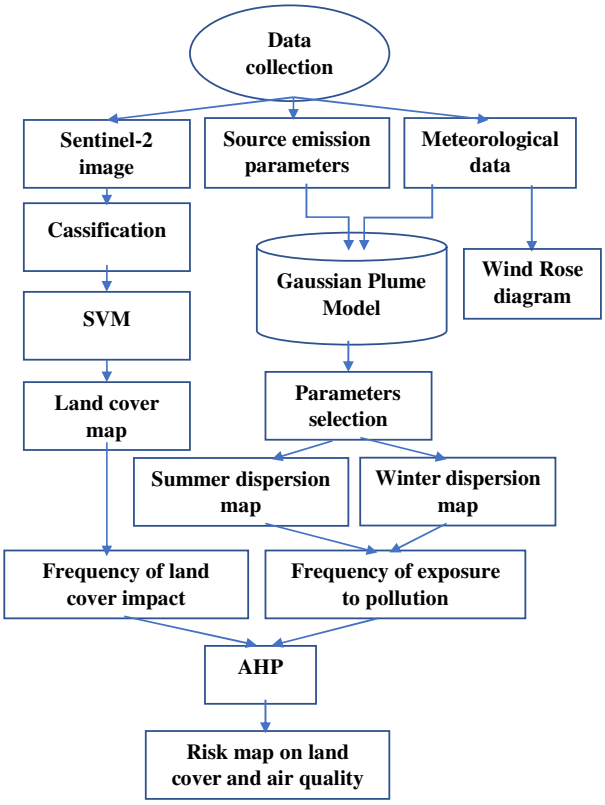

Fig. 4. The methodology applied in the research.

The classification of Kirkuk City is based on combining data on land use patterns, population distribution, and flaring site locations, using satellite imagery analysis and integrating meteorological data. Remote sensing and GIS techniques are employed to distinguish between residential areas, industrial facilities, and agricultural zones, while air quality measurement data supports the classification process.

The estimation process uses Pasquil-Gifford stability classes, wind speed data, and atmospheric conditions to generate concentration results at specific distances. By observing wind patterns, solar radiation during the day, and cloud cover at night, the Pasquill-Gifford stability classes are assigned. Properly selected stability classes are important for accurately calculating how gas disperses after flaring in Kirkuk. For instance, in the summer, on sunny and windy days, Class A–C (unstable) conditions help pollutants rise high. However, in winter, with little wind or clouds, more stable Class D–F conditions keep them closer to the ground. This results in a realistic illustration of dispersion across different seasons.

A. Classification Process

Kirkuk city was classified based on land use mapping, proximity to gas flaring sites, and meteorological conditions. This classification was performed using Sentinel-2 satellite images from 2024, along with meteorological data including wind speed and direction. Remote sensing, combined with GIS techniques, helps identify residential areas, industrial zones, and agricultural regions, enabling better land use planning and environmental zoning. Monitoring stations also provide on-site air pollution data to support the classification results. Here, we used the ArcGIS software for classification purposes. The method employed is Support Vector Machine (SVM). The study area was categorized into four types: residential buildings, vegetation, bare land, and water. The equation representing this method is as follows [31].

$$f(x) = sign\left(\sum_i^r \propto_i y_i k(x, x_i) + b\right) \quad (1)$$

where *αi (i*=1,..., *r)* are the Lagrange multipliers, *k (x, xi)* is the kernel function, *b* is the hyperplane's offset from the origin, *xi* is the feature vector for the *ith* training instance, representing its spectral response, *yi* is the class label corresponding to *xi*

B. Dispersion Modeling

Air pollution models can be categorized into three main categories: deterministic, statistical, and physical [32]. Deterministic models primarily rely on numerical approximation methods, such as finite difference and finite element techniques, to solve the partial differential equations that describe the physical process of atmospheric dispersion. These models are most useful for long-term planning [33]. Meanwhile, statistical models estimate ambient air concentrations through empirical relationships between meteorological and other relevant parameters. This approach is especially effective for short-term concentration predictions [32]. Physical models, on the other hand, simulate real processes in laboratory settings through experiments that replicate the key features of the phenomenon under study [34].

A gas flaring pollution dispersion model utilizes Gaussian Plume principles, integrated with Pasquil-Gifford stability categories and dispersion components. Scientists need to identify the primary gas flaring sites and quantify the emission rates of pollutants such as SO_2, NO_2, and PM. The simulation incorporates meteorological data such as wind speed, atmospheric stability, and temperature to model pollutant dispersion. Once the location of the flaring site, emission rate, stack height, wind speed, wind direction, atmospheric stability class, mixing height during the study, and related parameters are identified, the model equation can be used to estimate the expected pollutant dispersion downwind. Using GIS to map dispersion findings helps identify affected zones and assess risks to both nature and human health. The equation describing this model can be expressed as [35]:

$$C(x,y,z) = \frac{Q}{2\pi u \sigma_y \sigma_z} exp\left(-\frac{y^2}{2\sigma_y^2}\right)\left[exp\left(-\frac{(z-H)^2}{2\sigma_z^2}\right) + exp\left(-\frac{(z+H)^2}{2\sigma_z^2}\right)\right] \quad (2)$$

where *C(x, y, z)* represents the concentration of the pollutant at a specific point, *Q* denotes the emission rate of that pollutant, and *u* is the wind speed, $\sigma_y \sigma_z$ are the dispersion coefficients in the lateral (*y*) and vertical (*z*) directions, respectively, which depend on the downwind distance (x) and atmospheric stability. *H* represents the effective stack height (the actual height with plume rise).

C. GIS-Based Risk Mapping

The system utilizes GIS technology to create detailed maps of air pollution risk zones. GIS visualizes environmental hazards through spatial analysis in the final stage of the process. AHP ranks areas by evaluating pollution exposure levels and intensity along with vulnerability factors [36-37]. Risk spatial mapping techniques create visual representations of high-, medium-, and low-risk zones, supporting both environmental decision-making and administrative actions.

The fundamental equation of the AHP is [38]:

$$A * w = \lambda max * w \quad (3)$$

where *A* is, the matrix of pairwise evaluation, *w* is the priority vector, and λmax is the main eigenvalue of A.

V. RESULTS AND DISCUSSION

A. Classification Results

SVM classification is an analytical method used in GIS for remote sensing tasks and spatial data analysis. Users begin by collecting geospatial data. Preprocessing involves removing noise and normalizing features. Next, they select relevant attributes such as spectral bands, elevation, and vegetation indices. The SVM model trains to categorize data by finding an optimal boundary that distinguishes different land or terrain classes. Improving SVM models involves selecting the optimal training datasets and incorporating additional spatial layers to enhance analysis. Figure 5 shows the SVM map of the study area. The study area has been classified into three categories based on the region's characteristics: Bare land, Residential, and Vegetation.

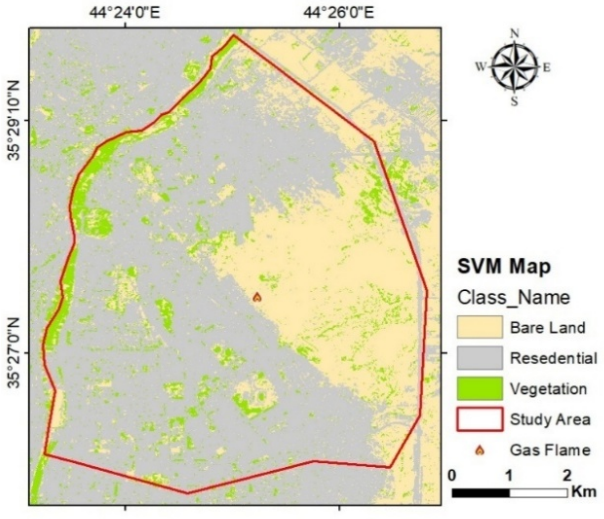

Fig. 5. SVM map of study area, Kirkuk City.

B. Dispersion Model Results

Maps of air pollutants were generated based on the flame position using the GPM equation. Model parameters were calculated separately for the summer and winter seasons. The equation was applied twice, and Table II shows the statistics of the Gaussian Dispersion Model (GDM). Figures 6 and 7 depict Gaussian dispersion for summer and winter, respectively. All pollutant concentrations, measured in µg/m³, were analyzed at 100m intervals along the flame. Dispersion effects notably diminish after 1 to 2 km, with concentrations becoming negligible beyond that distance. As shown in Figure 6, PM2.5 dispersion starts with a high concentration near the flame at 100 m, approximately 8216.60 µg/m³. The highest concentrations were found within a 300 m radius, indicating unhealthy air conditions.

TABLE II. GDM STATISTICS.

	Summer time		**Winter time**	
Distance from source	σ_y 0.22* y0.91	σ_z 0.2* y0.86	σ_y 0.16* y0.90	σ_z 0.12* y0.85
100m	14.53	10.49	10.09	6.01
200m	27.31	19.05	18.83	10.84
300m	39.50	26.99	27.13	15.30
400m	51.32	34.57	35.15	19.54
1000m	118.14	76.03	80.18	42.57
2000m	222.003	138.01	149.63	76.74

PM10 was also observed to be unhealthy air near the flame within 200m, ranging from 3286.64 to 64.53 µg/m^3. Beyond 300m to 2km, there is no impact from dispersion. Based on World Health Organization (WHO) standards, the air quality was unhealthy within 100m to 200m of the flame, with levels exceeding 200 µg/m³ for NO_2 and 500 µg/m³ for SO_2. Based on Figure 7, the concentrations were lower than those observed in summer. The dispersion of PM2.5 and PM10 extended 200m. Unhealthy air remains concentrated near the flame location at (100 to 200) m, while NO_2 and SO_2 were concentrated at 100m.

It is essential to recognize that seasonal changes can impact wind patterns, temperature, and air stability, all of which influence how pollutants disperse. For example, summer heat often helps lift fumes higher into the atmosphere, while winter cold tends to keep them close to the ground. This model presumes stable environmental and weather conditions, meaning it does not account for significant topographical changes or abrupt weather shifts. Additionally, a sensitivity analysis was conducted to gain a deeper understanding of the model's outputs. Under optimal conditions, the GPM typically produces errors ranging from 30% to 50% compared to actual values. A variation in Q by ±10% causes a change in concentration by approximately the same percentage in the same direction. Wind speed has the opposite effect on dispersion; a 20% change in wind speed can lead to variations in concentrations of 20% to 30%. Moreover, a change in stability can substantially alter ground-level concentrations. Even small increases in height have a significant impact on the amount of toxic gas near the ground. The basic parameter (wind speed) in the study is adjusted in the sensitivity analysis to understand its role in the model results. We changed (wind speed) by +20%, and the result was a -16.6%. This indicates that an increase in wind speed causes a 16.6% decrease in pollution levels. Wind speed works inversely with the dispersal of pollution. Wind speed and direction rarely stay the same as assumed in the GPM. This change can incorrectly show how pollutants disperse in areas with many structures. Due to these limitations, pollution levels are often underestimated, especially when the weather is unstable.

C. Resultant Risk Maps

In air quality analysis, a pairwise comparison reveals how environmental risk is prioritized across different distance intervals. Table III indicates that the 0-100 meters zone has the highest rating for air quality assessment, as its values are given more importance than those of other areas. Increasing the distance to 1000-2000 meters correlates with a reduction in environmental impact, suggesting a lower influence on air quality near pollution sources. The values in the early columns reflect higher air quality impacts at shorter distances from the source, which decreases as the distance from the point source grows. Analyzing these results helps scientists determine the percentage contribution of each air pollution distance range to environmental health risks. The AHP pairwise relationships of land cover (Table IV) indicate that urban areas present the most significant risk compared to other regions, including barren land. Vegetation falls between urban areas and barren land in terms of its influence on risk assessment. According to Table III, the risk criteria barren areas stand as the category with the minimum risk influence. The obtained weights demonstrate how urban areas tend to intensify environmental risks, including both heat and cold stress situations. The matrix underlies the procedure for calculating normalized weights, which appear in risk maps.

Table V displays the frequency of land cover impacts. The weights from the analysis total 1.0, showing that the categories have been compared equally. Environmental criteria have different weights across the three land cover types, where in this study, Urban is 0.545, Vegetation is 0.364, and Barren is 0.091, as shown in Table IV. The weight assigned to urban land cover types is 0.545, indicating they have the most significant effect. The weight of 0.364 for vegetation reflects its moderate impact on environmental criteria. Barren land has the least environmental impact because it carries the lowest weight of 0.091 compared to the other land types. The data on pollution exposure frequencies, distributed by distance intervals, are presented in Table VI. Dispersion exposes people to pollution, with the peak occurring within 100 meters of pollution sites, because the weighting factor is 0.458. The exposure levels decrease substantially as the distance increases, reaching their minimum point at approximately 1000–2000 meters (0.62 miles).

TABLE III. PAIRWISE COMPARISON OF AIR QUALITY

Criteria	**0-100m**	**100-200m**	**200-300m**	**300-400m**	**400-1000m**	**1000-2000m**
0- 100	1	2	4	6	8.5	9
100-200	0.5	1	2	3	4.5	5
200-300	0.25	0.5	1	2	2.5	3
300-400	0.16	0.33	0.5	1	1.5	2
400-1000	0.11	0.22	0.4	0.6	1	2
1000-2000	0.11	0.2	0.3	0.5	0.5	1
Sum	2.145	4.25	8.23	13.16	18.5	22

TABLE IV. PAIRWISE COMPARISON OF LAND COVER

Criteria	Urban	Vegetation	Barren
Urban	1	1.5	6
Vegetation	0.666667	1	4
Barren	0.166667	0.25	1
Sum	1.833333	2.75	11

TABLE V. FREQUENCY OF LAND COVER IMPACT

Criteria	Urban	Vegetation	Barren	Weights
Urban	0.54	0.54	0.54	0.545455
Vegetation	0.36	0.36	0.36	0.363636
Barren	0.09	0.09	0.09	0.090909
Sum				1

TABLE VI. FREQUENCY OF POLLUTION EXPOSURE.

Criteria	0-100	100-200	200-300	300-400	400-1000	1000-2000	Weights
0-100	0.46	0.46	0.48	0.45	0.45	0.409	0.457693
100-200	0.23	0.23	0.24	0.22	0.24	0.227	0.234886
200-300	0.11	0.11	0.12	0.15	0.13	0.136	0.129812
300-400	0.07	0.07	0.06	0.07	0.08	0.090	0.077446
400-1000	0.05	0.05	0.04	0.05	0.05	0.090	0.058539
1000-2000	0.05	0.04	0.04	0.03	0.02	0.045	0.041621
Sum							1

Furthermore, Figures 8 and 9 display the risk maps for land cover and air quality during the summer and winter seasons. This assessment employs the AHP methodology to evaluate various factors associated with decision-making regarding environmental and health risks from air pollution and land cover. In Figure 8, risk levels are categorized into three levels using a color gradient, with red indicating the highest risk, corresponding to the most vulnerable areas. Yellow represents Medium Risk, indicating intermediate vulnerabilities, and blue indicates Low Risk, representing the least vulnerable zones. The research area displays high-risk red zones mainly along the western central sections. This is influenced by environmental conditions such as urban density, lack of green cover, and higher surface temperatures. The western and southern parts are medium-risk areas, forming a protective ring around the high-risk (red) zones. Low-risk areas, indicated in blue, are primarily located in the eastern part of the map, characterized by favorable conditions such as increased vegetation, improved wind flow, and cooler temperatures. The eastern region's low risk may be due to smart city planning, extensive green spaces, and open areas that help reduce heat buildup.

In Figure 9, cyan indicates low-risk zones, light blue shows medium-risk areas, and pink marks high-risk zones on the winter risk map. The most hazardous regions (pink) cluster mainly in central zones and west of the city center. High-risk zones are bordered by medium-risk zones (light blue) that extend from their edges into central and western areas. The eastern and southeastern regions mostly contain low-risk zones (cyan), indicating lower vulnerability. Western and central regions maintain high risk levels year-round, both in winter and summer. The eastern area consistently stays low-risk, likely due to favorable urban or environmental factors. The high-risk zones expand during summer, while in winter, they are more localized in central areas. Both maps display similar risk patterns, as they are based on the same weighting scheme, with minor differences resulting from variations in pollutant concentrations.

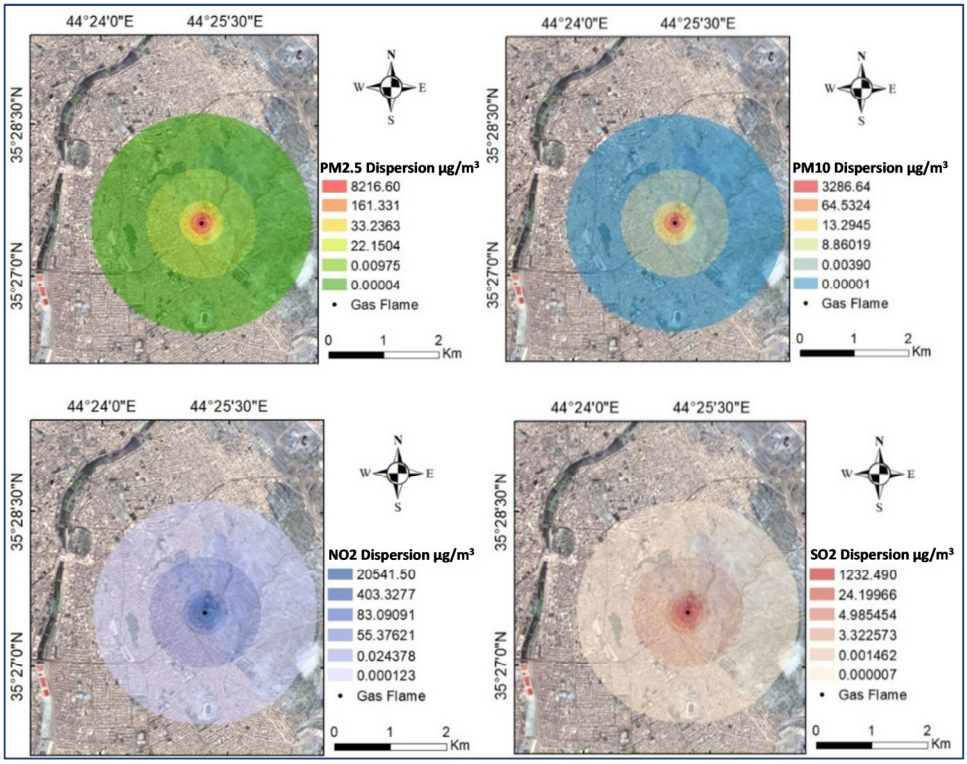

Fig. 6. Pollutant dispersion in summer.

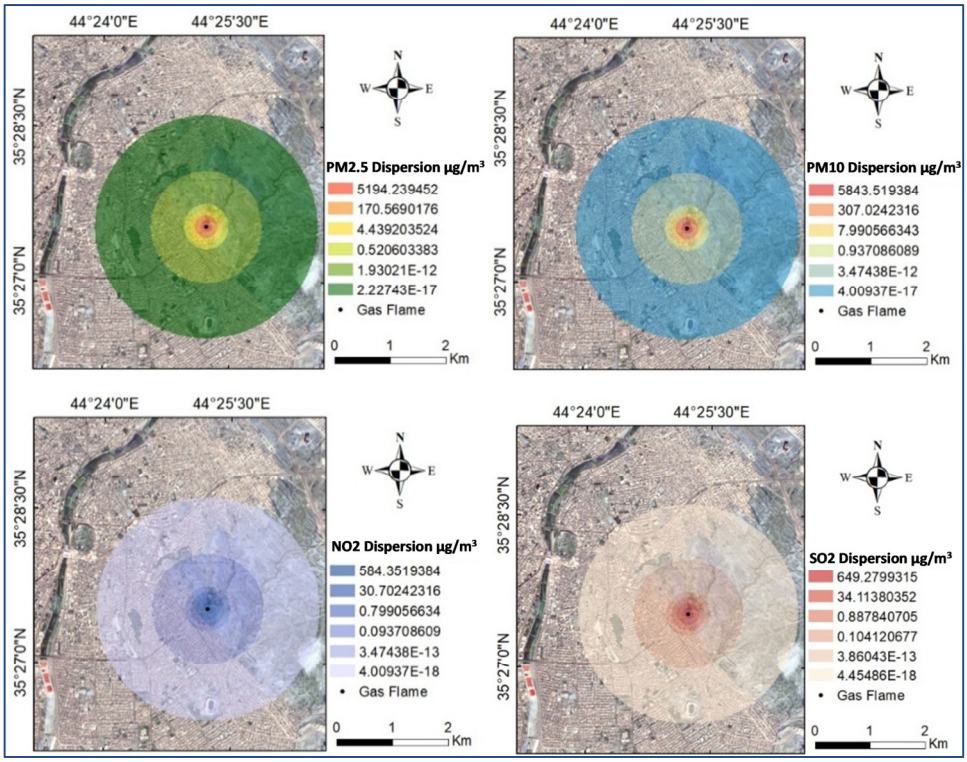

Fig. 7. Pollutant dispersion in winter

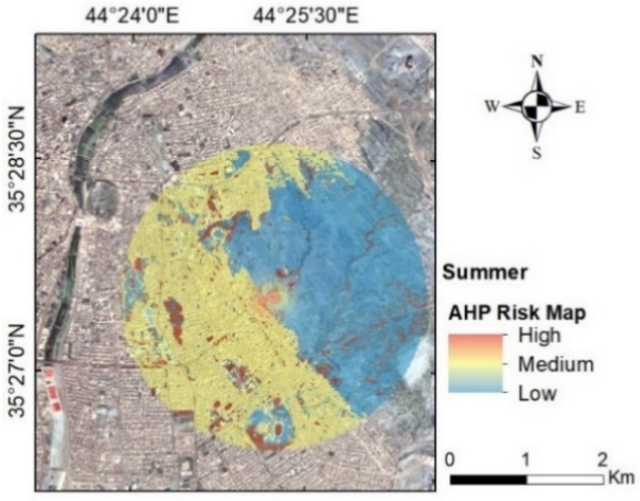

Fig. 8. Risk map on land cover and air quality in summer.

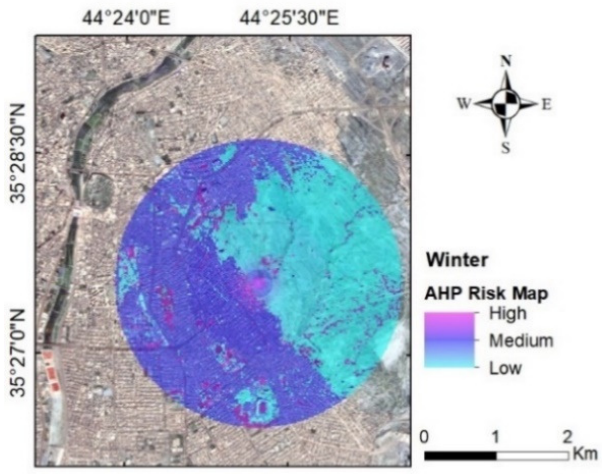

(b)

Fig. 9. Risk map on land cover and air quality in winter.

Compared to WHO standards, the accepted daily average PM2.5 is 15 µg/m³, with an annual average of 5 µg/m³ [39], whereas the U.S. Environmental Protection Agency (USEPA) sets these limits at 35 µg/m³ and 12 µg/m³, respectively [40]. The WHO establishes a limit of 200 µg/m³ for NO_2 for up to 1 hour, and the USEPA sets it at 188 µg/m³ (100 ppb) [41]. Integrating GIS and remote sensing has proven to be very significant [42], while environmental pollution is considered by [42].

VI. CONCLUSION

This research reveals how gas flaring contributes to significant pollution-related environmental issues in Kirkuk City. It utilizes a combination of GIS techniques, the Gaussian Plume Dispersion Model, and the Analytical Hierarchy Process (AHP) to identify pollution patterns and affected areas effectively. Pollutant levels reach their highest near flaring sites, while weather conditions and atmospheric stability influence the spread of pollutants. AHP maps reveal a consistent risk pattern across the city, especially in the western

and central regions. The east remains relatively safe through seasonal changes. Variations in pollutant levels cause slight shifts in the distribution pattern. These findings highlight that proper planning and ample green spaces lead to cleaner air. Sustainable environmental improvements depend on gas recovery systems and flaring reduction programs for effective emission control. Ongoing research and technology development are essential to balance industrial activities with environmental protection. The study recommends the use of advanced technologies to achieve an industrial-environmental balance. Policy changes to address flaring are crucial for improving urban air quality and public health, aligning with Goal 11 of the Sustainable Development Goals and Iraq's National Environmental Action Plan. Implementing these strategies supports nationwide efforts to cut greenhouse gases and fulfill Goal 13. Protecting land, green spaces, and the air enhances overall environmental sustainability.

ACKNOWLEDGMENT

The authors would like to thank Dr. Qayssar Mahmoud Ajaj from the Northern Technical University for his help with some analyses in this study.

REFERENCES

[1] A. G. Aregbe, "Natural Gas Flaring—Alternative Solutions," *World Journal of Engineering and Technology*, vol. 5, no. 1, pp. 139–153, Dec. 2016, https://doi.org/10.4236/wjet.2017.51012.

[2] S. H. Saleh and A. F. Hassoon, "Assessment of Air Pollutants for Baba Industrial Area at Kirkuk Oil Field, Iraq," *The Iraqi Geological Journal*, pp. 125–137, Nov. 2024, https://doi.org/10.46717/igj.57.2E.10ms-2024-11-19.

[3] M. Faruolo, A. Caseiro, T. Lacava, and J. W. Kaiser, "Gas Flaring: A Review Focused On Its Analysis From Space," *IEEE Geoscience and Remote Sensing Magazine*, vol. 9, no. 1, pp. 258–281, Mar. 2021, https://doi.org/10.1109/MGRS.2020.3007232.

[4] E. G. Nisbet *et al.*, "Methane Mitigation: Methods to Reduce Emissions, on the Path to the Paris Agreement," *Reviews of Geophysics*, vol. 58, no. 1, Mar. 2020, Art. no. e2019RG000675, https://doi.org/10.1029/2019RG000675.

[5] R. Mills, "A new hope: Iraq oil's way forward," *Al-Bayan Center Publications Series*, Iraq, 2018.

[6] N. Obi, "Study of the Impact of gas flaring on the health of communities in Delta region of Nigeria," Ph.D. dissertation, School of Dentistry & Medical Sciences, Faculty of Science, Charles Sturt University, Sydney, Australia, October 2021.

[7] P. Robinson, "Safety and the Environment," in *Springer Handbook of Petroleum Technology,* Hsu, C.S., Robinson, P.R., Eds. Springer International Publishing, 2017; pp. 85–147.

[8] H. H. Hamed *et al.*, "Predicting PM2.5 levels over the north of Iraq using regression analysis and geographical information system (GIS) techniques," *Geomatics, Natural Hazards and Risk*, vol. 12, no. 1, pp. 1778–1796, Jan. 2021, https://doi.org/10.1080/19475705.2021.1946602.

[9] J. K. Nduka, V. N. Okafor, and I. O. Odiba, "Impact of Oil and Gas Activities on Acidity of Rain and Surface Water of Niger Delta, Nigeria: An Environmental and Public Health Review," *Journal of Environmental Protection*, vol. 7, no. 4, pp. 566–581, Mar. 2016, https://doi.org/10.4236/jep.2016.74051.

[10] M. Mardani, M. Nowrouzi, and H. Abyar, "Assessing the environmental impact of offshore flares in the Persian Gulf: A comprehensive analysis of SO2 emissions," *Advances in Environmental Technology*, vol. 11, no. 1, pp. 63–74, Jan. 2025, https://doi.org/10.22104/aet.2024.6494.1781.

[11] T. Elbir, "A GIS based decision support system for estimation, visualization and analysis of air pollution for large Turkish cities," *Atmospheric Environment*, vol. 38, no. 27, pp. 4509–4517, Sep. 2004, https://doi.org/10.1016/j.atmosenv.2004.05.033.

[12] V. Yadav and R. Ganguly, "Evaluation and Spatial Mapping of Criteria Air Pollutants in an Industrial City in India," *Journal of Hazardous, Toxic, and Radioactive Waste*, vol. 29, no. 3, Jul. 2025, Art. no. 04025011, https://doi.org/10.1061/JHTRBP.HZENG-1450.

[13] A. A. Kuta, S. Grebby, and D. S. Boyd, "Remote Monitoring of the Impact of Oil Spills on Vegetation in the Niger Delta, Nigeria," *Applied Sciences*, vol. 15, no. 1, Jan. 2025, Art. no. 338, https://doi.org/10.3390/app15010338.

[14] H. Jamal Jumaah, A. Jasim, A. Rashid, and Q. Ajaj, "Air Pollution Risk Assessment Using GIS and Remotely Sensed Data in Kirkuk City, Iraq," *Journal of Atmospheric Science Research*, vol. 6, no. 3, pp. 41–51, Aug. 2023, https://doi.org/10.30564/jasr.v6i3.5834.

[15] A. Zoeir, J. Qajar, Y. Kazemzadeh, E. Khodapanah, and A. Rastkar, "To optimize gas flaring in Kirkuk refinery in various seasons via artificial intelligence techniques," *Scientific Reports*, vol. 13, no. 1, Aug. 2023, Art. no. 13406, https://doi.org/10.1038/s41598-023-40724-2.

[16] G. K. A. Sada and T. W. M. Salih,"Enhancing Indoor Air Quality for Residential Building in Hot-Arid Regions," in *Sustainable Building for a Cleaner Environment*, A. A. Aziz El-Batsh, Ed. Springer, 2018, pp. 255–264, https://doi.org/10.1007/978-3-319-94595-8_21.

[17] H. J. Jumaah and K. V. Kamran, "AQI-based box model using GIS and remote sensing over Kirkuk city, Iraq," *Advanced Engineering Days*, vol. 9, pp. 144–146, 2024.

[18] H. J. Jumaah, M. H. Ameen, S. Mahmood, and S. J. Jumaah, "Study of air contamination in Iraq using remotely sensed Data and GIS," *Geocarto International*, vol. 38, no. 1, Feb. 2023, Art. no. 2178518, https://doi.org/10.1080/10106049.2023.2178518.

[19] S. Ali, M. Najemaden, and R. Ahmed, "Using GIS techniques for mapping the pollution of particulate materials in Kirkuk," *Sustainable Resources Management Journal*, vol. 3, no. 2, pp. 58–66, 2018.

[20] S. Mahmood, A. Ali, and H. J. Jumaah, "Geo-visualizing the hotspots of smog-induced health effects in district Gujranwala, Pakistan: a community perspective," *Environmental Monitoring and Assessment*, vol. 196, no. 5, Apr. 2024, Art. no. 457, https://doi.org/10.1007/s10661-024-12619-w.

[21] M. R. Mahmood, B. I. Abrahem, H. J. Jumaah, H. A. Alalwan, and M. M. Mohammed, "Drought monitoring of large lakes in Iraq using remote sensing images and normalized difference water index (NDWI)," *Results in Engineering*, vol. 25, Mar. 2025, Art. no. 103854, https://doi.org/10.1016/j.rineng.2024.103854.

[22] H. J. Jumaah, M. H. Ameen, B. Kalantar, H. M. Rizeei, and S. J. Jumaah, "Air quality index prediction using IDW geostatistical technique and OLS-based GIS technique in Kuala Lumpur, Malaysia," *Geomatics, Natural Hazards and Risk*, vol. 10, no. 1, pp. 2185–2199, Jan. 2019, https://doi.org/10.1080/19475705.2019.1683084.

[23] H. J. Jumaah, A. A. Rashid, S. A. R. Saleh, and S. J. Jumaah, "Deep Neural Remote Sensing and Sentinel-2 Satellite Image Processing of Kirkuk City, Iraq for Sustainable Prospective," *Journal of Optics and Photonics Research*, Aug. 2024, https://doi.org/10.47852/bonviewJOPR42022920.

[24] M. H. Ameen *et al.*, "Evaluation of PM2.5 Particulate Matter and Noise Pollution in Tikrit University Based on GIS and Statistical Modeling," *Sustainability*, vol. 13, no. 17, Jan. 2021, Art. no. 9571, https://doi.org/10.3390/su13179571.

[25] Q. Ajaj, N. Awad, H. Jumaah, and H. Rizeei, "Air quality regrssion analysis over Iraq during severe dust periods using GIS and remotely sensed PM2.5," *DYSONA - Applied Science*, vol. 6, no. 2, pp. 300–308, 2025.

[26] N. Sharma, K. Bhandari, P. Rao, και A. Shukla, "GIS applications in air pollution modeling," *Geospatial World*, 2003.

[27] L. O. Uche and O. Azoro-Amadi, "Aligning Nigeria's International Obligations: A Comprehensive Analysis of Environmental Protection within the Industrial Law and Policy Framework," *South African Yearbook of International Law*, vol. 49, Apr. 2024, https://doi.org/10.25159/2521-2583/15159.

[28] S. S. Shah and Z. Asghar, "Individual attitudes towards environmentally friendly choices: a comprehensive analysis of the role of legal rules, religion, and confidence in government," *Journal of Environmental Studies and Sciences*, vol. 14, no. 4, pp. 629–651, Dec. 2024, https://doi.org/10.1007/s13412-024-00913-5.

[29] A. E. Esiri, O. A. Babayeju, I. O. Ekemezie, A. E. Esiri, O. A. Babayeju, and I. O. Ekemezie, "Implementing sustainable practices in oil and gas operations to minimize environmental footprint," *GSC Advanced Research and Reviews*, vol. 19, no. 3, pp. 112–121, 2024, https://doi.org/10.30574/gscarr.2024.19.3.0207.

[30] P. Simpa, N. O. Solomon, O. A. Adenekan, and S. C. Obasi, "Environmental stewardship in the oil and gas sector: Current practices and future directions," *International Journal of Applied Research in Social Sciences*, vol. 6, no. 5, pp. 903–926, May 2024, https://doi.org/10.51594/ijarss.v6i5.1132.

[31] H. J. Jumaah, M. H. Ameen, and B. Kalantar, "Surface Water Changes and Water Depletion of Lake Hamrin, Eastern Iraq, Using Sentinel-2 Images and Geographic Information Systems," *Advances in Environmental and Engineering Research*, vol. 4, no. 1, pp. 1–11, Jan. 2023, https://doi.org/10.21926/aeer.2301006.

[32] S. Srivastava and I. N. Sinha, "Classification of air pollution dispersion models: A critical review," in *Proceedings of National Seminar on Environmental Engineering with special emphasis on Mining Environment (NSEEME-2004)*, Dhanbad, India, Mar. 19–20, 2004.

[33] H. G. Matthies, "Stochastic finite elements: Computational approaches to stochastic partial differential equations," *ZAMM - Journal of Applied Mathematics and Mechanics*, vol. 88, no. 11, pp. 849–873, Nov. 2008, https://doi.org/10.1002/zamm.200800095.

[34] Y. Tominaga and T. Stathopoulos, "Ten questions concerning modeling of near-field pollutant dispersion in the built environment," *Building and Environment*, vol. 105, pp. 390–402, Aug. 2016, https://doi.org/10.1016/j.buildenv.2016.06.027.

[35] Q. Mahmood Ajaj, H. Z. M. Shafri, A. Wayayok, and M. Firuz Ramli, "Assessing the Impact of Kirkuk Cement Plant Emissions on Land cover by Modelling Gaussian Plume with Python and QGIS," *The Egyptian Journal of Remote Sensing and Space Science*, vol. 26, no. 1, pp. 1–16, Feb. 2023, https://doi.org/10.1016/j.ejrs.2022.12.001.

[36] W. Prommachan, P. Surin, P. Srinoi, and M. Pipathattakul, "Selection Criteria for Evaluating Predictive Maintenance Techniques for Rotating Machinery using the Analytic Hierarchical Process (AHP)," *Engineering, Technology & Applied Science Research*, vol. 14, no. 1, pp. 13058–13065, Feb. 2024, https://doi.org/10.48084/etasr.6816.

[37] N. Kumar and R. Jha, "GIS-based Flood Risk Mapping: The Case Study of Kosi River Basin, Bihar, India," *Engineering, Technology & Applied Science Research*, vol. 13, no. 1, pp. 9830–9836, Feb. 2023, https://doi.org/10.48084/etasr.5377.

[38] A. Kebede, D. Sintayehu, N. Tessema, B. Girma, and J. Yousuf, "Drought vulnerability characterization and nature-based adaptation, Eerer Sub-Basin, Eastern Ethiopia," *Ethiopian Journal of Science and Sustainable Development*, vol. 12, no. 1, pp. 64–81, 2025.

[39] G. B. Stanojević *et al.*, "Spatio-temporal variability of annual PM2. 5 concentrations and population exposure assessment in Serbia for the period 2001-2016," *Journal of the Geographical Institute "Jovan Cvijić" SASA*, vol. 69, no. 3, pp. 197–211, Dec. 2019, https://doi.org/10.2298/IJGI1903197S.

[40] K. Walters, J. Jacobson, Z. Kroening, and C. Pierce, "PM2.5 Airborne Particulates Near Frac Sand Operations," *Journal of Environmental Health*, vol. 78, no. 4, pp. 8–12, 2015.

[41] T. Lindvall, "Recommendations for air quality standards for nitrogen dioxide and ozone," *Scandinavian Journal of Work, Environment & Health*, vol. 11 Suppl 3, pp. 3–9, 1985.

[42] T. M. E. Nthaga, T. Nyomboi, and M. Mwaniki, "An Integrated Remote Sensing and GIS Road Condition Assessment Framework: Applying Geospatial Techniques to Improve Pavement Condition Analysis," *Engineering, Technology & Applied Science Research*, vol. 15, no. 2, pp. 21021–21028, Apr. 2025, https://doi.org/10.48084/etasr.9785.